https://doi.org/10.5194/egusphere-2026-4734
Preprint. Discussion started: 21 August 2026

Forecasting the 12 November 2019 Venice *Acqua Alta* event: the role of baroclinic compounding effects

Anna Chiara Goglio[1,2], Emanuela Clementi[1], Nadia Pinardi[2], Giulio Boccaletti[1], Paolo Oddo[2], Lorenzo Mentaschi[2]

[1] CMCC Foundation - Euro-Mediterranean Center on Climate Change, Bologna, Italy
[2] Alma Mater Studiorum - University of Bologna, Bologna, Italy

Correspondence to: A.C. Goglio (annachiara.goglio@cmcc.it)

Abstract. The northern Adriatic Sea is known to be threatened by extreme sea level events. Venice is exposed to these events, locally known as *Acqua Alta*, which cause the flooding of the historical city centre. Despite its relevance, a comprehensive analysis of extreme *Acqua Alta* events that considers all possible compounding drivers, including baroclinic contributions, is, to our knowledge, still missing. In this work, numerical results based on the *Copernicus Marine Mediterranean Analysis and Forecasting System* are analyzed to better understand the physical mechanisms underlying the 12 November 2019 *Acqua Alta* event and to assess individual processes playing a role in the event dynamics.
The novel finding of this study is the identification of the contribution of baroclinic dynamics. We estimate a net baroclinic contribution of 7 cm (4 %) to the 175 cm sea level peak. We show for the first time that internal seiches along the northern Adriatic slope contribute to the dynamics of the *Acqua Alta* event. Moreover, we identify a northern Adriatic density front and quantify its contribution to the time-mean positive northward sea level slope.

1 Introduction

The Adriatic Sea (northern Mediterranean Sea) is an area affected by extreme sea level events, which have become more severe and frequent in recent decades (Faranda et al., 2023). Given the high population density along the basin, these events pose a significant risk, making accurate forecasting a challenging but crucial tool for mitigating their socio-economic impacts.

The Adriatic Sea is a semi-enclosed basin located between the Italian and the Balkan peninsulas connected to the Mediterranean Sea through the Otranto Strait. It is characterized by shallow bathymetry (average depth of 126 m) and a channel-like shape (Fig. 1a). This region represents a hotspot for extreme sea level events in the Mediterranean Sea (Cid et al., 2016; Marcos et al., 2009). The complexity of sea level extremes dynamics in this area is often regarded as a representative example for the study of coastal floods in a broader global context (Ferrarin et al., 2022).

The historical city centre of Venice stands out as one of the areas most exposed to sea level flooding, locally called *Acqua Alta* events, typically occurring during the autumn season. Events characterized by a sea level peak exceeding 140 cm are classified as *extreme floods* by Venice Municipality (Official Venice Municipality webpage on *Acqua Alta* events

https://doi.org/10.5194/egusphere-2026-4734
Preprint. Discussion started: 21 August 2026

https://www.comune.venezia.it/en/content/venice-and-high-water, last access: 4 August 2026). This water level corresponds to the flooding of 60 % of Venice's historical city centre (Cavaleri et al., 2020). Since the implementation of the MoSE barrier system (Leonardi, 2021; Official MoSE website https://mosevenezia.eu, last access: 4 August 2026), the focus has shifted towards supporting timely decisions on barrier activation (Umgiesser and Matticchio, 2006; Pirazzoli, 2002; Faranda et al., 2023).

In this work, the 12 November 2019 event is analyzed. During this event, the water level recorded at the *Institute of Marine Sciences Acqua Alta Platform* (ISMAR Tide-gauge official website https://www.comune.venezia.it/it/content/3-piattaforma-ismar-cnr, last access: 4 August 2026) offshore the Venice Lagoon (*I-TG* in Fig. 1b) reached 182 cm (Giesen et al., 2021), corresponding to a 175 cm hourly mean value. The flood covered 85 %–90 % of the historical city centre (Cavaleri et al., 2020). The damages associated with this exceptional event were estimated to be 460 million euros (Godlewski et al., 2020).

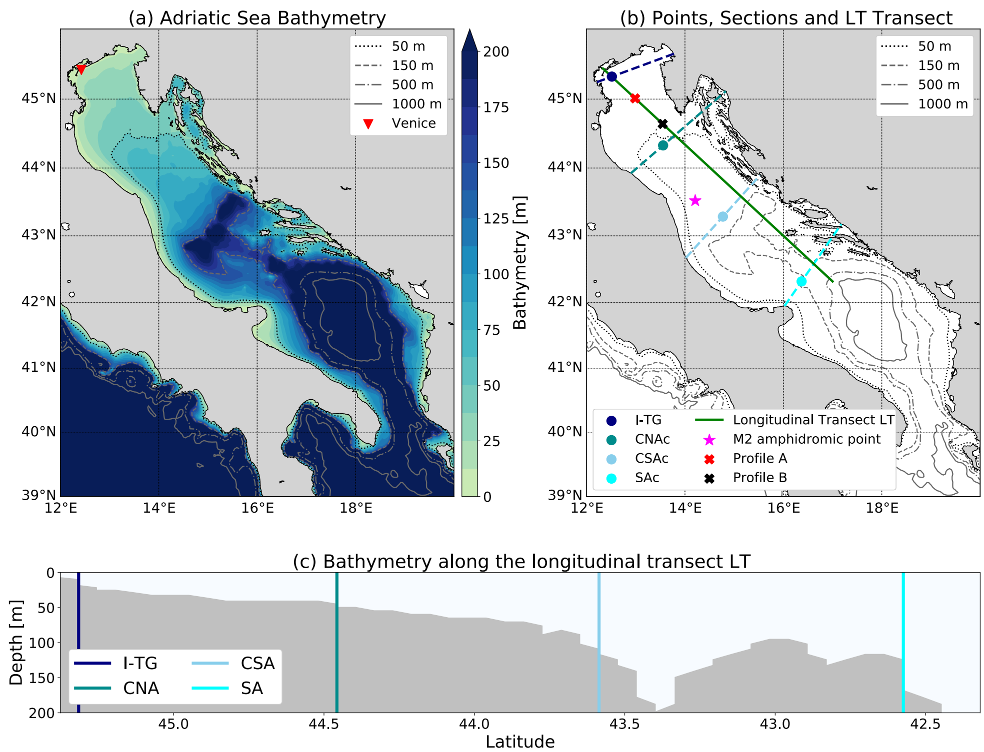

Figure 1. (a) MedFS Adriatic Sea bathymetry and Venice city centre location (red triangle). (b) I-TG, SAc, CNAc, CSAc points and sections location (coloured circles and corresponding dashed lines), vertical A and B profiles location (red and black crosses) and LT longitudinal transect (green line) used by the analyses presented in this work. The semidiurnal M2 tidal amphidromic point is also shown (magenta star). Bathymetric contours corresponding to 50, 150, 500, and 1000 m are superimposed. (c) Bathymetry along longitudinal transect LT from north to south and intersection of LT with the dashed sections shown in the map of panel (b) (vertical coloured lines).

Lionello et al. (2021a) and Ferrarin et al. (2022) recognized that Venice *Acqua Alta* events are compound events resulting from the superimposition of several drivers: meteorological surge, tides, seiches, seasonal and long-term sea level changes.

https://doi.org/10.5194/egusphere-2026-4734
Preprint. Discussion started: 21 August 2026

Meteorological conditions are the primary drivers (Giesen et al., 2021; Faranda et al., 2023), leading to extreme floods especially when occurring in phase with high tides (Lionello et al., 2021b) and pre-existing seiches (Robinson et al., 1973). Extreme low-pressure patterns, and the Scirocco wind blowing along the main axis of the basin toward Venice, play a crucial role in generating storm surges in the northern parts of the basin, and amplifying barotropic seiches (Cavaleri et al., 2020; Trincardi et al., 2016). The uncertainty associated with atmospheric forcings is known to represent the main limitation to the predictability of *Acqua Alta* events (Umgiesser et al., 2021; Wang et al., 2021; Ferrarin et al., 2021; Giesen et al., 2021).
The barotropic contributions to *Acqua Alta* events, including surges, tides and seiches, have been extensively analyzed in the past (Lionello et al., 2021b; Umgiesser et al., 2021). Recently, Ferrarin et al. (2023) found that the extreme atmospheric low-pressure event of 12 November 2019 also excited oscillations at meteotsunami frequencies. These processes non-linearly interact, and the importance of such interactions has been highlighted by several studies (Idier et al., 2019; Woodworth et al., 2019). In particular, McDonagh et al. (2024) showed resonances between tides and seiches in the Mediterranean basin. In fact, the first two oscillatory eigenmodes of the Adriatic basin have periods close to those of the dominant tidal constituents in the basin, the diurnal K1 component and the semidiurnal M2 and S2 components (Vilibić et al., 1998), resulting in resonant amplification.

Giesen et al. (2021) showed that the forecast from the operational *Copernicus Marine Mediterranean Analysis and Forecasting System* (MedFS, Coppini et al., 2023) predicted the 12 November 2019 sea level peak with 20 % error three days in advance. In this study, we revisit the 12 November 2019 *Acqua Alta* event to investigate the baroclinic contributions, which have not yet been elucidated. For the global ocean, Wang et al. (2021) showed that baroclinic processes contribute to total water level across the entire frequency spectrum, and Wang et al. (2022) found that including baroclinicity in a global storm surge forecasting model improves predictions of total water level. Additionally, it is well established that baroclinic models improve the representation of the tidal signal by accounting for barotropic–baroclinic energy conversions (Arbic et al., 2010; Borile, 2022).

The objective of this paper is to use the MedFS operational system and a barotropic version of the same ocean model to analyze the compounding drivers that led to the 12 November 2019 *Acqua Alta* event. We begin by validating the model against local sea level data and then isolate specific processes to assess their individual contributions to the event. The primary focus is on the role of baroclinic dynamics. The main aim is to improve the understanding of physical mechanisms underlying these extreme sea level events, with the goal of improving their predictability.

The analysis considers re-forecasting experiments forced by ECMWF atmospheric forcings, using barotropic and baroclinic model formulations, with and without tides, all initialized three days ahead of the *Acqua Alta* event that occurred on the 12 November 2019 at 21:00 UTC.

The paper starts with a brief description of the data and methods used in this work. Sect. 3 analyzes the different elements of the 12 November 2019 *Acqua Alta* compound event. The novel findings introduced by our study are described in Sect. 3.3 where the baroclinic contributors are treated. Sect. 4 presents the discussion, and Sect. 5 the conclusions.

https://doi.org/10.5194/egusphere-2026-4734
Preprint. Discussion started: 21 August 2026

2 Data and methods

A set of re-forecast experiments based on the *Copernicus Marine Mediterranean Analysis and Forecasting System*, all initialized on 10 November 2019, is used to analyze the 12 November 2019 *Acqua Alta* event. We focused on the three-day forecast because, according to operational procedures, several days are needed for the timely management of the MoSE system (Umgiesser and Matticchio, 2006). Moreover, beyond the third day the available atmospheric forcing has a lower temporal resolution.

The experiment referred to as MedFS is forced with ECMWF atmospheric forecasts at the highest available spatial and temporal resolution, namely 1/10 of a degree and 1 hour, and explicitly accounts for the eight main tidal components. MedFS-NT is a MedFS twin experiment without tides. A barotropic implementation of the numerical model on the same horizontal grid, called MedFS-BT, is also considered. Model sea level outputs are saved as hourly averages. System settings are detailed in Appendix A.

Numerical results are compared with hourly in situ observations recorded during November 2019 by the ISMAR tide-gauge (*I-TG* in Fig. 1b). The offset applied to the modelled time series is obtained by shifting each curve to align the three-day mean over the 10–12 November 2019 period to the observed mean at ISMAR tide-gauge.

In situ data are also used to validate the individual components of the modelled sea level at ISMAR tide-gauge extracted from the total sea level as follows. A decomposition to extract the individual barotropic contributions to the sea level anomaly with respect to the 1–12 November 2019 time-mean is applied to hourly time series obtained by concatenating the analysis on which the forecasts are initialized with the 10–12 November 2019 three-day forecast. The tidal signal is extracted by harmonic analysis using the *ttide* package (Pawlowicz et al., 2002). The seiche signal is obtained from the detided time series by means of a band-pass filter tuned to two frequency bands covering the two main Adriatic oscillatory modes, namely [19.0, 22.3] hours and [9.9, 11.8] hours. These two bands were defined in a preliminary sensitivity analysis to minimize the difference between the seiches extracted from the system runs with and without tides.

The main limitation to the accuracy of this analysis arises from the limited length of the input time series, which results in a low spectral resolution leading to uncertainty in the separation between the tidal and the oscillatory modes. In particular, the diurnal tidal frequencies are close to the first Adriatic oscillatory mode resonance (Vilibić et al., 1998), and the semi-diurnal tides are close to the second Adriatic oscillatory mode. Moreover, as discussed in the Introduction, tides and oscillatory modes interact. Therefore, in this study we present a joint tides–seiches signal which includes the signal belonging to two bands covering both diurnal and semi-diurnal peaks. The residual signal includes the storm surge component and the high-frequency sea level oscillations. These oscillations may include higher-order oscillatory modes, meteotsunamis, and local resonance contributions.

https://doi.org/10.5194/egusphere-2026-4734
Preprint. Discussion started: 21 August 2026

3 Results

The sea level time series recorded at the ISMAR tide-gauge (navy line in Fig. 2) shows the extreme sea level peak associated with the *Acqua Alta* event that occurred on 12 November 2019 around 21:00 UTC. From about 18:30 to 22:00 UTC (grey area in Fig. 2), the sea level exceeded the 140 cm extreme flood threshold (dashed red line in Fig. 2).

During the 10–12 November 2019 period, the mean sea level reached 76 cm. Due to the atmospheric conditions and the associated storm surge, the mean sea level over the whole month of November 2019 was 67 cm, corresponding to twice the annual mean sea level of 34 cm (Cavaleri et al., 2020; Ferrarin et al., 2021).

Both MedFS and MedFS-BT re-forecasts initialized at 00:00 UTC on 10 November 2019 (green and orange lines in Fig. 2) successfully predict the *Acqua Alta* event three days in advance, with an error of 18 cm and 25 cm relative to the observed peak sea level of 175 cm, i.e. ~10 % and 14 % error respectively. Therefore, although the barotropic model predicts the event, it underestimates the peak by 7 cm compared with the baroclinic forecast. We interpret the 7 cm difference between MedFS and MedFS-BT at peak as an estimate of the contribution of baroclinic processes to the *Acqua Alta* event. This contribution is discussed in Sect. 3.3.

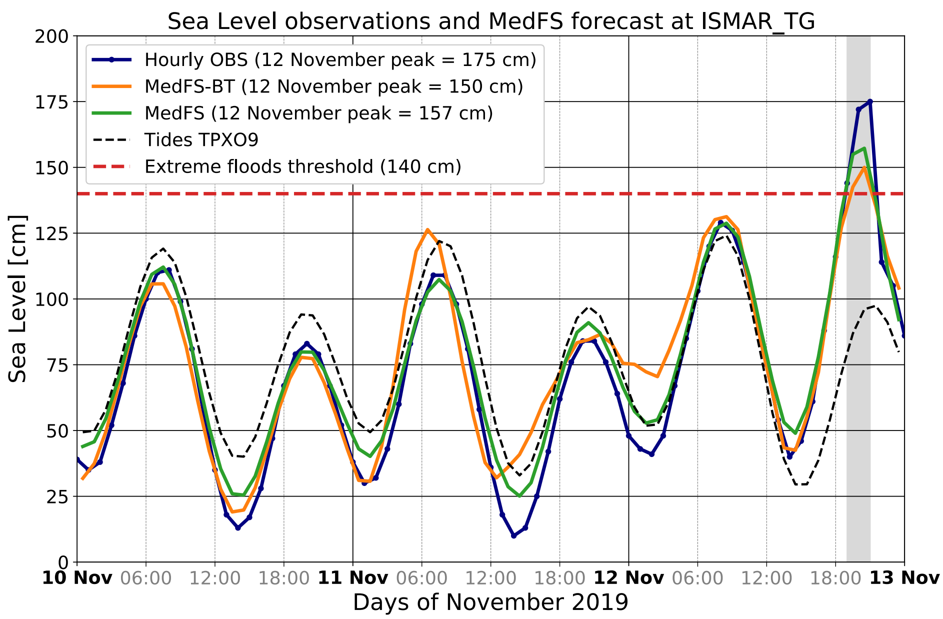

Figure 2. MedFS (green line) and MedFS-BT (orange line) sea level re-forecasts initialized on 10 November 2019 at 00:00 UTC compared to hourly sea level record at ISMAR tide-gauge (navy line). Hourly tidal signal (black dashed line) extracted from the nearest grid point in the TPXO9 global barotropic model (Egbert and Erofeeva, 2002). The extreme floods threshold (dashed red line) and the *Acqua Alta* event of 12 November 2019 (grey area) are highlighted.

https://doi.org/10.5194/egusphere-2026-4734
Preprint. Discussion started: 21 August 2026

3.1 Atmospheric forcing contribution

The atmospheric conditions around the 12 November 2019 event have been extensively described in the literature (Ferrarin et al., 2021; Giesen et al., 2021). A deep low-pressure system over the central-southern Tyrrhenian Sea generated a strong Scirocco wind blowing along the main axis of the Adriatic basin, while a smaller but intense local cyclone reached Venice at 20:30 UTC (Ferrarin et al., 2021; Cavaleri et al., 2020). Giesen et al. (2021) found that the mean ECMWF wind speed, used to force the MedFS operational forecast system, was almost 10 m s^{-1} lower than the Advanced SCATterometer (ASCAT, Stoffelen et al., 2017) wind speed. Cavaleri et al. (2020) estimated a 5 hPa difference between the pressure recorded at the ISMAR oceanographic tower and the ECMWF MSL pressure field. Moreover, Ferrarin et al. (2021, 2023) analyzed in detail the sensitivity of this event to the path and intensity of the small-scale cyclone in the Northern Adriatic and found that the exact position of the depression was critical to reach the high-water peak. All these previous results demonstrate that most of the sea level forecast error for the 12 November 2019 event is connected to the atmospheric forcing uncertainty.
To qualitatively test the sensitivity of the MedFS re-forecast to the ECMWF atmospheric forcings accuracy, several numerical experiments forced by a decreased spatial and/or temporal atmospheric forcing resolution have been carried out in a preliminary phase. The outcomes show that, on average, the increase in ECMWF fields spatial resolution from 1/8 to 1/10 of a degree has a negligible effect on the results, whereas the temporal frequency of the forcing is crucial to reproduce the 157 cm sea level peak (see Table A2 in Appendix A), which is consistent with the findings of Wang et al. (2021) for the global ocean.

3.2 Barotropic contributions

An analysis of tides, seiches, storm surge, and high-frequency fluctuations contributions to the sea level anomaly associated with the 12 November 2019 peak has been applied to the MedFS re-forecast.
Considering the TPXO tidal signal (Egbert and Erofeeva, 2002) at ISMAR tide-gauge (black dashed line in Fig. 2), it can be noted that the high sea level peak occurred during the low high tide phase, as described for other events that occurred in different areas of the coastal ocean (Idier et al., 2019; Williams et al., 2016). The tidal amplitude during this tidal phase is about 25 cm lower than the higher high tide recorded a few hours in advance. Therefore, in the case of 12 November 2019, the contribution of tides to the sea level peak is lower than in events characterized by the coincidence of the storm surge and the higher high tide, such as the 22 November 2022 *Acqua Alta* event (Boetti et al., 2026). Nevertheless, the 12 November 2019 event represents the second maximum ever recorded in Venice (Giesen et al., 2021), second only to the 1966 event (1.94 m; Trincardi et al., 2016), suggesting that Venice is potentially subject to even more extreme water levels.
By filtering the time series as described in Sect. 2, the temporal evolution of the tides–seiches signal and of the residual component during the three-day period is derived from the sea level anomaly time series. Figure 3 shows the map of the sea level anomaly (Fig. 3a) and of the individual contributions (Fig. 3b and Fig. 3c) at the time of the sea level maximum, i.e.

https://doi.org/10.5194/egusphere-2026-4734
Preprint. Discussion started: 21 August 2026

20:30 UTC on 12 November 2019. Both components are shown to positively contribute to the sea level peak in the northern Adriatic, with a slightly larger contribution from the residual component.

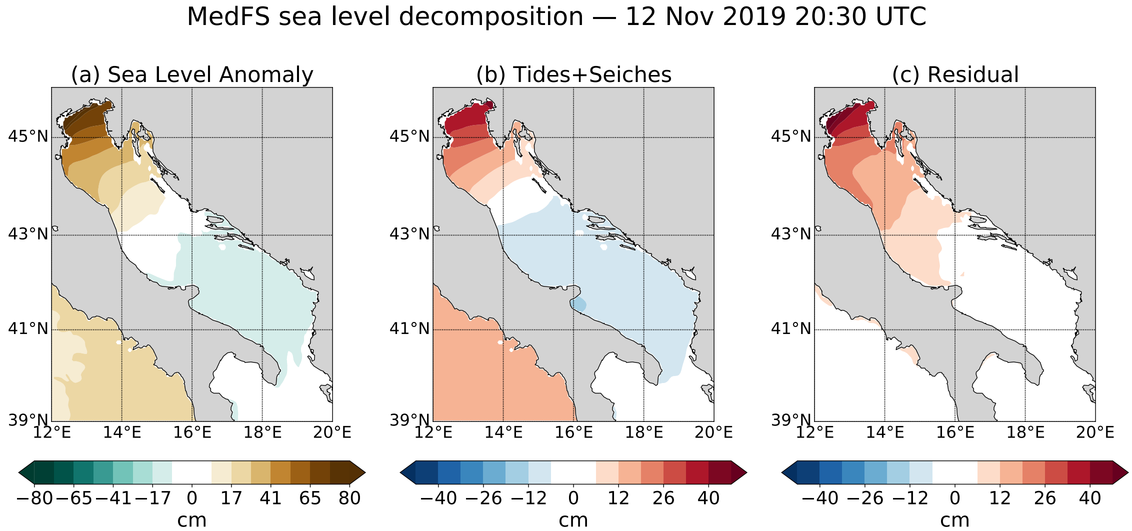

Figure 3. (a) Sea level anomaly during the *Acqua Alta* event at 20:30 UTC on 12 November 2019 from MedFS re-forecast. Decomposition of the sea level anomaly into (b) tides–seiches and (c) residual contributions.

By extracting the temporal evolution of the sea level anomaly at the ISMAR tide-gauge (Fig. 4) we evaluate the weight of these components to the sea level peak. Analyzing the sea level values recorded during the 12 November 2019 event (navy lines in Fig. 4), 80 cm of the total measured sea level can be attributed to the surge and high-frequency contributions, 32 cm to tides and seiches oscillations.

MedFS re-forecast (green lines in Fig. 4) reproduces the observed components, with the largest discrepancy associated with the residual component. The underestimation of the atmospheric forcing component, which drives the surge, likely explains this discrepancy.

MedFS-BT residual exhibits an amplitude underestimation of 7 cm at peak with respect to MedFS, while the MedFS-BT tides and seiches signal shows a comparable amplitude with respect to MedFS. These results support the conclusion of a non-negligible contribution from baroclinic processes to the event. The MedFS-BT residual shows a high-frequency component characterized by a period around 8 hours more energetic than in MedFS during the day preceding the *Acqua Alta* peak. This may be related to a different response of the barotropic model to the wind forcing associated with the wind speed intensification observed in the day preceding the *Acqua Alta* event (Giesen et al., 2021), as in the barotropic configuration the energy cannot be redistributed through internal modes.

https://doi.org/10.5194/egusphere-2026-4734
Preprint. Discussion started: 21 August 2026

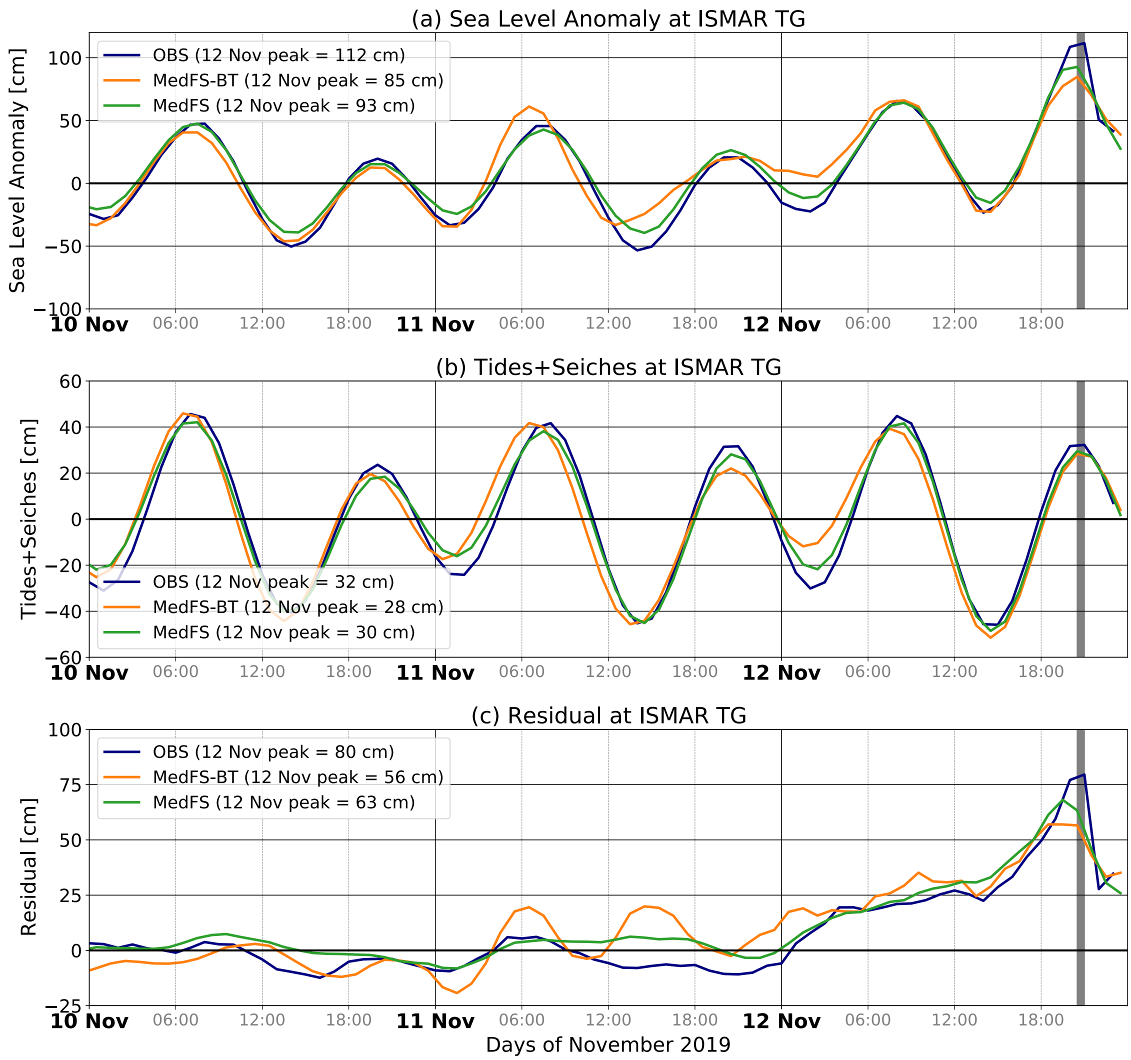

185 **Figure 4.** (a) Sea level anomaly, (b) tides–seiches contribution and (c) residual contribution during the 10–12 November 2019 period at ISMAR tide-gauge extracted from observed values (navy line), MedFS re-forecast (green line) and MedFS-BT re-forecast (orange line). The *Acqua Alta* sea level peak is highlighted (grey area).

3.3 Baroclinic contributions

190 To investigate the baroclinic dynamics associated with the *Acqua Alta* event, baroclinic currents are analyzed across the whole Adriatic basin and compared with their barotropic counterpart. Furthermore, we analyze the density field along the mid-Adriatic longitudinal transect (LT in Fig. 1b) and evaluate the terms of the barotropic sea level equation between the A and B profiles (A and B in Fig. 1b) located along the transect.

https://doi.org/10.5194/egusphere-2026-4734
Preprint. Discussion started: 21 August 2026

3.3.1 Internal seiches

An assessment of the velocity field is carried out at several locations distributed from the north to the centre of the Adriatic Sea along the main axis of the basin (circle markers of Fig. 1b). Only the current components oriented toward Venice (north-westward), normal to the transversal sections shown in Fig. 1b (dashed lines) are considered.

The barotropic current, $\bar{\vec{u}}$, is extracted from the total horizontal velocity field, $\vec{u}$, computing the vertical average:

$$\bar{\vec{u}} = \frac{1}{H+\eta} \int_{-H}^{\eta} \vec{u} \, dz \qquad (1)$$

The baroclinic component is defined as $\vec{u}' = \vec{u} - \bar{\vec{u}}$.

Figure 5 shows the temporal evolution during the three-day re-forecast of the MedFS barotropic and baroclinic currents at the four control points of Fig. 1b (I-TG, CNAc, CSAc, SAc). The sign convention is positive for currents directed northward, and negative for southward ones.

The baroclinic velocity vertical structure (Fig. 5e–h) is characterized by a dominant first baroclinic mode with additional components from the second and third internal vertical modes. In the southernmost section SAc (Fig. 5h) the second and third baroclinic modes have higher amplitude, which gradually decreases toward the north.

The northern shelf slope section CNAc (Fig. 5f) shows an anomalous baroclinic amplitude. In this location the barotropic currents have maximum amplitude (Fig. 5b) and the baroclinic current zero crossing is located near the bottom (Fig. 5f), a signature of bottom pressure compensation due to sloping bathymetry as described by Mellor and Wang (1996).

Baroclinic current amplitudes become comparable with the barotropic ones a few hours before the event. The intensification occurs first at the CSAc point which is located in the Middle Adriatic where bathymetry changes from 200 m to 50 m depth. We argue that in this area internal seiches are generated or amplified by the conversion of barotropic potential energy into baroclinic kinetic energy along the topography (Arbic, 2022).

https://doi.org/10.5194/egusphere-2026-4734
Preprint. Discussion started: 21 August 2026

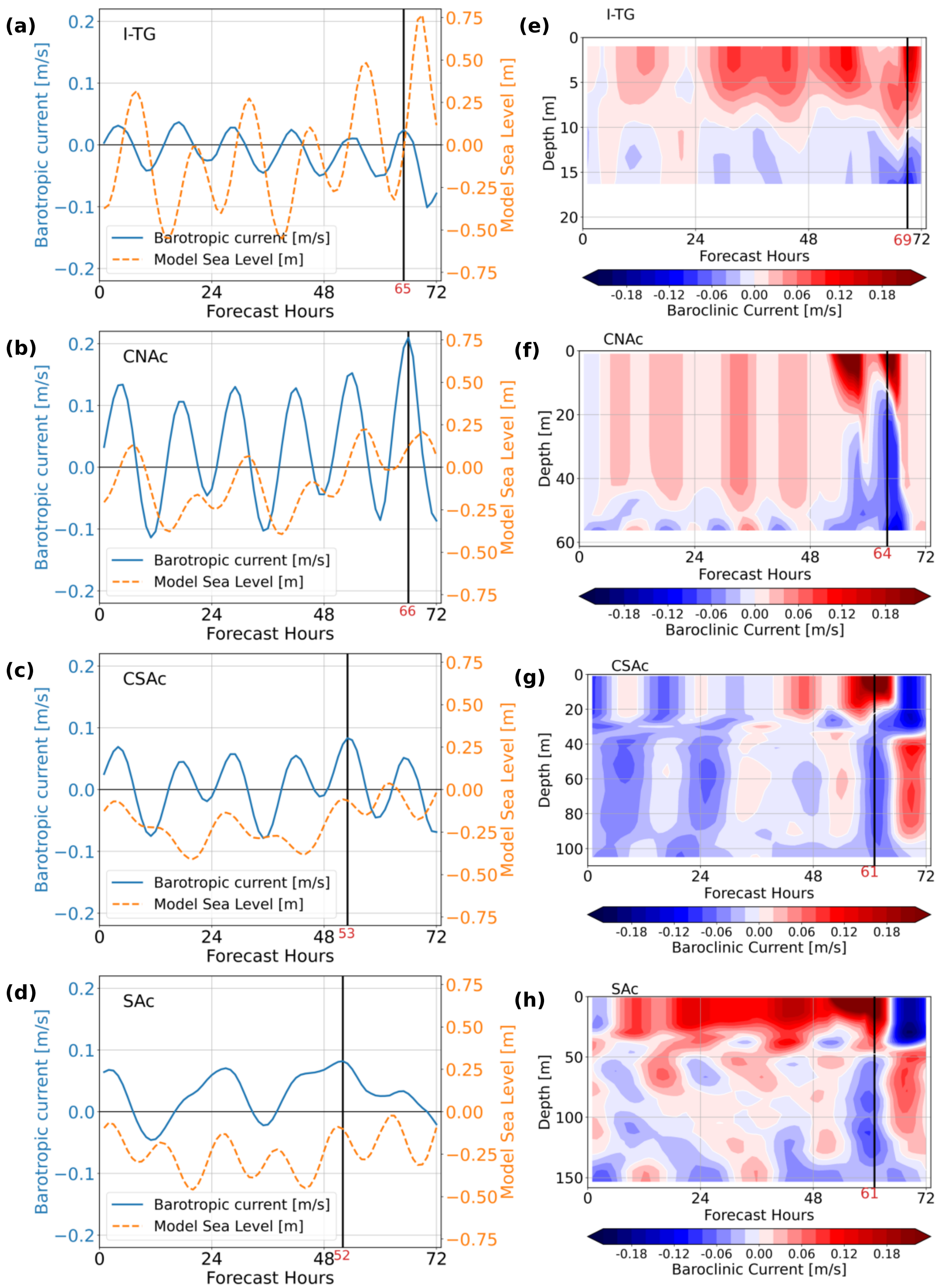

215 **Figure 5.** Left column (a–d): sea level (orange dashed line) and barotropic currents (blue line) time series at the locations indicated in Fig. 1b. Right column (e–h): Hovmöller depth-time plots of baroclinic current components at the locations indicated in Fig. 1b. All the plots refer to the MedFS re-forecast initialized on 10 November 2019 and cover the 10–12 November 2019 period (0–72 hours). The time of maximum current amplitude is highlighted by a vertical black line.

https://doi.org/10.5194/egusphere-2026-4734
Preprint. Discussion started: 21 August 2026

To demonstrate the presence of internal seiches, the MedFS re-forecast is compared with the results obtained from the system version without tides, MedFS-NT. The time evolution of the barotropic and baroclinic currents at the CSAc point is shown for the simulation without tides in Fig. 6. Internal waves are detected in both tidal and non-tidal cases (Fig. 5g and Fig. 6b), demonstrating the existence of internal seiches with a period of about 12 hours. Moreover, the amplitude of baroclinic waves is modified in the non-tidal case, providing evidence that baroclinic seiches interact with internal tides. We conclude that internal seiches, generated along the northern Adriatic slope, are a major component of the baroclinic current dynamics associated with the *Acqua Alta* sea level event.

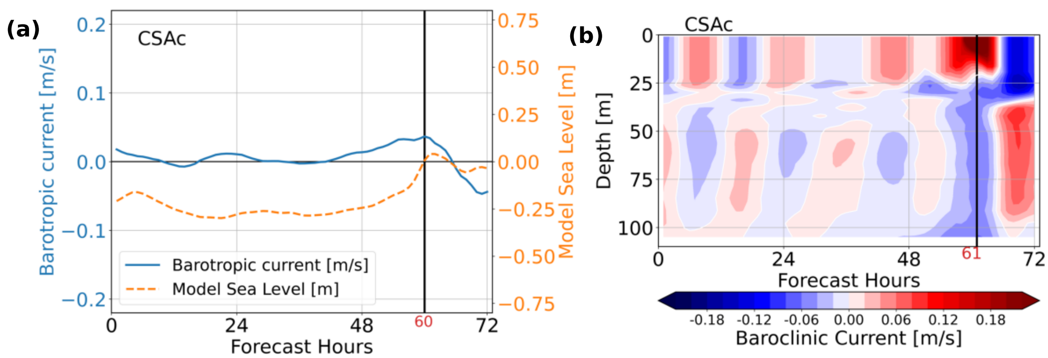

Figure 6. (a) Sea level (orange dashed line) and barotropic currents (blue line) time series, and (b) baroclinic currents Hovmöller depth-time plots. The time series are obtained from MedFS-NT re-forecast. The black vertical lines correspond to the instant of the maximum current value. Both plots of the Figure refer to CSAc location and are obtained from the non-tidal re-forecast initialized on 10 November 2019 and covering the 10–12 November 2019 period.

3.3.2 North Adriatic density front

Similarly to the case of the tidal mixing front described by Dong et al. (2018) for the Georges Bank region, we analyze how the baroclinic density structure influences the barotropic sea level in the northern Adriatic Sea.

The Adriatic Sea density front is a known feature of the general circulation of the Adriatic basin (Zavatarelli and Pinardi, 2003; Oddo et al., 2005). The large-scale cyclonic circulation of the basin is characterized by the branching of the northward eastern Adriatic current into two currents, one of which hugs the shelf break around 44.8° N. The frontal region is shown in Fig. 7b along the northern portion of the longitudinal transect LT (green line in Fig. 7c). The density front is bottom intensified and, as shown by Davies and Xing (2002), can be associated with the generation of inertial internal waves.

The two profiles delimiting the front (A and B in Fig. 7c) bound the along-front cyclonic current. The relevance of the baroclinic components to the sea level between these profiles in the frontal area (Fig. 7b) is analyzed using the linearized, steady state momentum equation as in Dong et al. (2018):

https://doi.org/10.5194/egusphere-2026-4734
Preprint. Discussion started: 21 August 2026

$$f\bar{u} = -\frac{1}{\rho_0}\frac{\partial \overline{p_{atm}}}{\partial y} - g\frac{\partial \bar{\eta}}{\partial y} - \frac{\partial}{\partial y}\int_z^0 \left[g\,\frac{\bar{\rho}-\rho_0}{\rho_0}\right] dz' + \frac{1}{\rho_0}\left[\frac{\partial \overline{\tau_{yy}}}{\partial y} + \frac{\partial \overline{\tau_{yz}}}{\partial z}\right] \qquad (2)$$

where y is the along-transect direction, u is the cross-transect velocity, f is the Coriolis parameter, ρ is the density, ρ_0 is the reference density, $\overline{p_{atm}}$ is the atmospheric pressure and the overbar denotes a time averaging. In Eq. (2) the across-transect horizontal viscosity is neglected.

By integrating in vertical between the surface and the bottom, H, we obtain:

$$g\frac{\partial \bar{\eta}}{\partial y} = -\frac{1}{\rho_0}\frac{\partial \overline{p_{atm}}}{\partial y} - f\bar{u}_{BT} - g\frac{\partial}{\partial y}\int_{-H}^0 \left[\frac{\bar{\rho}-\rho_0}{\rho_0}\right] dz - \frac{g}{H}\frac{\partial}{\partial y}\int_{-H}^0 \left[\frac{\bar{\rho}-\rho_0}{\rho_0}\right] z\, dz + \frac{1}{H\rho_0}\int_{-H}^0 \frac{\partial \overline{\tau_{yy}}}{\partial y}\, dz + \frac{1}{\rho_0}\,\frac{\tau_{wind}-\tau_{bottom}}{H} \qquad (3)$$

where $\bar{u}_{BT} = \frac{1}{H}\int_{-H}^0 u\, dz$ is approximately the time averaged barotropic velocity field. τ_{wind} and τ_{bottom} are the wind and bottom stress respectively. The vertical integral is only computed between a flat surface and the bottom since we consider only a steady state balance and the free surface variations can be neglected to first order in the vertical integral. The baroclinic contribution to the meridional sea level slope (left hand side of Eq. (3)) is due to the fourth and the fifth terms in Eq. (3).

If we now integrate in the y direction between the A and B profiles (Fig. 7b), the contribution to the northward sea level gradient is:

$$\bar{\eta}_A - \bar{\eta}_B = +\overbrace{\frac{f}{g}\int_A^B \bar{u}_{BT}\, dy}^{1} + \overbrace{\int_{-H_B}^0 \frac{\bar{\rho}_B-\rho_0}{\rho_0}\, dz - \int_{-H_A}^0 \frac{\bar{\rho}_A-\rho_0}{\rho_0}\, dz}^{2} + \overbrace{\int_{-H_B}^0 \frac{\bar{\rho}_B-\rho_0}{\rho_0}\frac{z}{H_B}\, dz - \int_{-H_A}^0 \frac{(\bar{\rho}_A-\rho_0)}{\rho_0}\frac{z}{H_A}\, dz}^{3} +$$

$$-\overbrace{\frac{1}{g\rho_0}\left(\int_{-H_B}^0 \frac{\bar{\tau}_{yy}|_{y=B}}{H_B}\, dz - \int_{-H_A}^0 \frac{\bar{\tau}_{yy}|_{y=A}}{H_A}\, dz\right)}^{4} + \overbrace{\frac{1}{g\rho_0}\int_A^B \frac{\bar{\tau}_{wind}-\bar{\tau}_{bottom}}{H}\, dy}^{5} - \overbrace{\frac{1}{g\rho_0}\left(\overline{p_{atm\,A}} - \overline{p_{atm\,B}}\right)}^{6} \qquad (4)$$

The six terms on the right-hand side of Eq. (4) represent the dynamical balance giving rise to a sea level difference across the front between points A and B. Term 1 is the cross-transect barotropic transport, Terms 2 and 3 are the bottom pressure due to density and potential energy terms respectively (Mellor, 1996), Term 4 is the difference in the horizontal momentum stress across the front, Term 5 is the net wind and bottom stress contribution, and Term 6 is the atmospheric pressure difference across the front.

Analyzing the 10–12 November 2019 period, the mean sea level along the *LT* transect exhibits a positive slope (Fig. 7a), implying that some of the right-hand side terms in Eq. (4) positively contribute to this gradient and, consequently, to the *Acqua Alta* sea level event. The values of the terms relative to the MedFS forecast are reported in Table 1. Term 1, Term 2, Term 3, Term 5 and Term 6 are evaluated from MedFS outputs, while Term 4 is obtained as the residual from the others.

https://doi.org/10.5194/egusphere-2026-4734
Preprint. Discussion started: 21 August 2026

Table 1. Values of individual terms in Eq. (4) evaluated between profile *A* and profile *B* along *LT* longitudinal transect. All the terms except Term 4 are evaluated from MedFS re-forecast. Term 4 is obtained as the difference between the other terms of the equation.

Sea level difference across the front	**Term 1 Barotropic velocity across the front**	**Term 2 First baroclinic term contribution to sea level**	**Term 3 Second baroclinic term contribution to sea level**	**Term 4 Horizontal viscosity**	**Term 5 Net (wind-bottom) stress on the water column**	**Term 6 Atmospheric pressure difference across the front**
2.9 cm (Evaluated from MedFS results)	−0.4 cm (Evaluated from MedFS results)	3.4 cm (Evaluated from MedFS results)	0.9 cm (Evaluated from MedFS results)	−1.0 cm (Obtained as residual)	−0.2 cm (Evaluated from MedFS results)	0.2 cm (Evaluated from MedFS results)

The positive contributions to the 2.9 cm time-mean sea level across the front are the baroclinic terms and the atmospheric pressure. The baroclinic terms contribute up to 4.3 cm while the atmospheric pressure difference contribution is of the order of 0.2 cm. We can therefore conclude that the density-driven bottom pressure term (Term 2) and the potential energy term (Term 3) are the key processes contributing to the time-mean northward positive sea level slope. The cross-frontal current term has a net decreasing effect as for tidal mixing fronts in the Georges Bank Atlantic region (Dong et al., 2018), as well as the net, wind minus bottom, stress (Term 5) and the horizontal viscosity term (Term 4).

The dynamical balance described by Eq. (4) represents a mechanism through which bottom pressure and potential energy terms contribute to the mean sea level slope, enhancing the sea level at the coast. We argue that these baroclinic time-mean processes involve the internal seiches and tides described in the previous section.

https://doi.org/10.5194/egusphere-2026-4734
Preprint. Discussion started: 21 August 2026

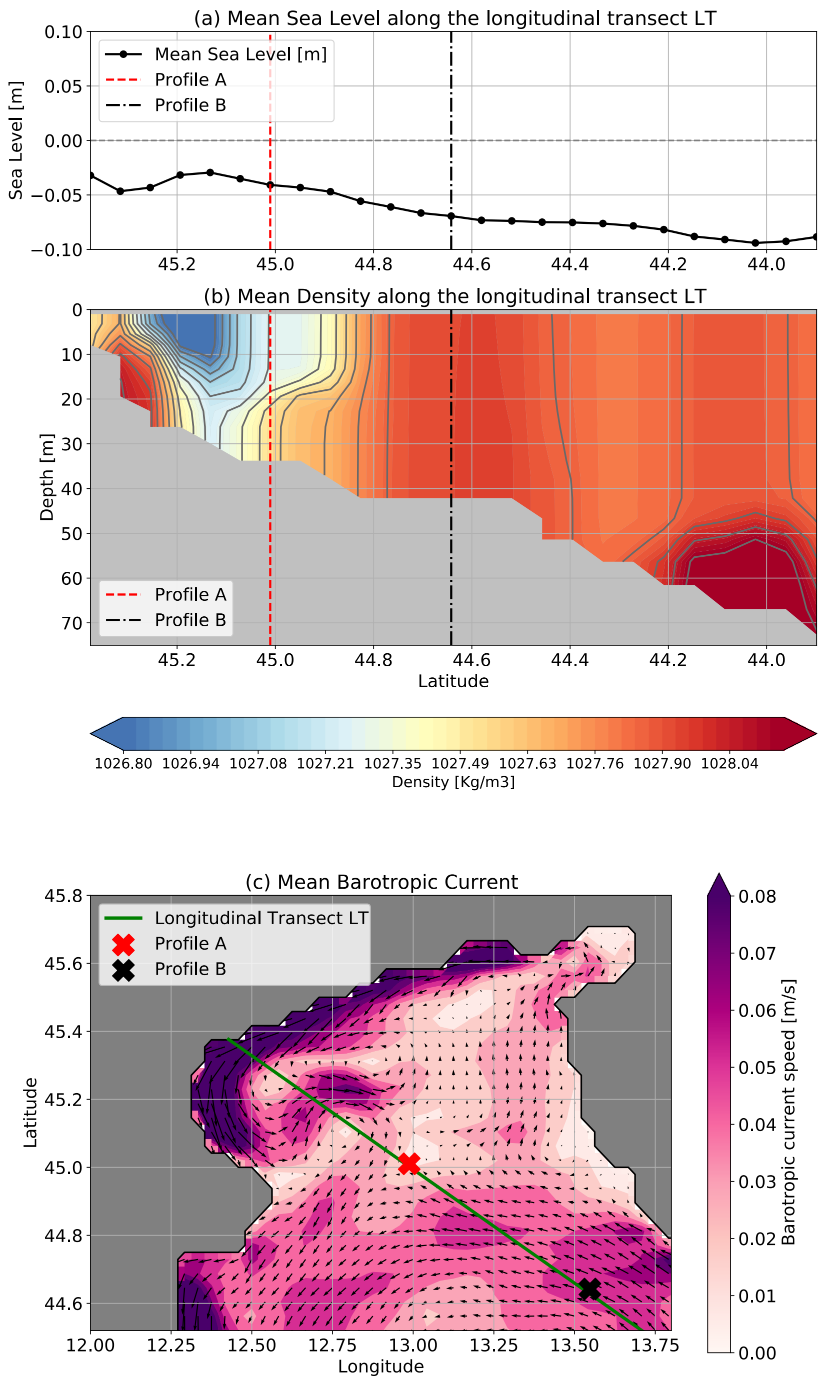

290 **Figure 7.** (a) Mean sea level and (b) mean density field along the longitudinal transect LT (green line in panel (c)). Grey lines in panel (b) are isopycnal contours. A and B profiles delimit the frontal region (red and black vertical lines respectively). (c) Mean barotropic current in the northern Adriatic area. Mean fields are obtained as averages over the 10–12 November 2019 three-day period from MedFS re-forecast.

https://doi.org/10.5194/egusphere-2026-4734
Preprint. Discussion started: 21 August 2026

4 Discussion

Investigating the role of baroclinic contributions in *Acqua Alta* events represents a novel aspect in the study of these phenomena. Internal waves in the Adriatic Sea have been considered in the literature (Vilibić and Orlić, 1999; McDonagh et al., 2026) but never associated with *Acqua Alta* events. Robinson et al. (1973) and Bajo et al. (2019) discuss the impacts of barotropic seiches on sea level extremes in the northern Adriatic, and our results are consistent with their findings. However, our analysis shows the existence of internal seiches generated along the northward sloping bottom of the Adriatic Sea during the *Acqua Alta* event.

Density fronts have been found to contribute to the positive slope between coastal and offshore sea levels. In this study we documented the existence of a bottom-intensified density front in the northern Adriatic Sea, which contributes to the positive northward three-day time-mean sea level slope across the northern shelf/slope interface.

MedFS is a basin-scale forecasting model with about 4 km resolution that is capable of forecasting the 12 November 2019 *Acqua Alta* event three days in advance, although it underestimates the sea level peak by 18 cm. The MedFS forecast underestimation has been previously associated with inaccuracies of the atmospheric forcing (Giesen et al., 2021).

Based on our results, we argue that representing the Adriatic basin internal dynamics, characterized by baroclinic seiches, their interaction with tides, and the northern Adriatic density front, may contribute to the skill of the MedFS forecast in predicting the *Acqua Alta* sea level peak of 12 November 2019. It is important to underline that baroclinic processes, contributing only about 4 % to the 12 November 2019 sea level peak, are not the main contribution to the three-day forecast skill, nor are they the dominant mechanism governing the event. Nevertheless, our results identify for the first time baroclinic dynamics as an additional compounding process contributing to the sea level peak.

5 Conclusions

Understanding the dynamics of *Acqua Alta* events is crucial for the timely operations of the defence barriers in the Venice Lagoon, to support the optimal management of barrier closures (Leonardi, 2021). The results discussed in this work provide further insight into this understanding.

The analysis presented in this paper provides evidence of how baroclinic processes contributed to the compound *Acqua Alta* event of 12 November 2019. We show evidence of baroclinic seiches non-linearly interacting with tides. Internal seiches are amplified along the northern Adriatic slope and generate first and second mode vertical baroclinic current structures. These resonant seiche modes intensify before and during the development of the extreme sea level event.

Furthermore, a bottom-intensified density front centred around 44.8° N is shown to contribute about 3 cm to the time-mean sea level increase in the northern Adriatic during the 10–12 November 2019 period. This represents a mechanism through which internal baroclinic potential energy contributes to sea level enhancement toward the coasts.

The fully baroclinic MedFS operational model better reproduces the sea level peak during the *Acqua Alta* event with respect to the barotropic system version MedFS-BT. The difference of 7 cm at the sea level peak between MedFS and MedFS-BT

https://doi.org/10.5194/egusphere-2026-4734
Preprint. Discussion started: 21 August 2026

represents an estimate of the contribution associated with baroclinic processes to the 12 November 2019 *Acqua Alta* sea level event, whose inclusion contributes to a more complete representation of the dynamics of these extreme events.

We conclude that the numerical model employed for the prediction of extreme sea level events should account for both barotropic and baroclinic processes, since baroclinic dynamics may represent an additional compounding process contributing to extreme sea level events, as shown in this work for the *Acqua Alta* event of 12 November 2019.

Moreover, the model domain should cover a region large enough to represent the development of all the involved dynamical processes. In particular, the representation of seiches is crucial and requires a numerical model capable of accurately representing basin modes with their characteristic frequencies and spatial structures. The *Copernicus Marine Mediterranean Analysis and Forecasting System*, with a domain covering the Mediterranean basin and an accurate representation of basin geometry and bathymetry, allows the representation of the relevant forcing mechanisms and oscillatory dynamics involved in the *Acqua Alta* event of 12 November 2019.

A possible extension of this work could be the analysis of the baroclinic contributions to other extreme sea level events that occurred in the Mediterranean basin, in which they might play an even more relevant role.

Appendix A: MedFS forecasting system

The analysis presented in this work is based on the *Mediterranean Analysis and Forecasting System* (MedFS), operational in the framework of the Copernicus Marine Service (Coppini et al., 2023). In particular, the version of the MedFS system used in this work (EAS9) is based on the NEMO v4.2 (Madec and the NEMO System Team, 2023) hydrodynamical model hourly coupled with WaveWatch-III v6.07 (WW3) wave model (WaveWatch III Development Group, 2019). Both models cover a domain that includes the whole Mediterranean Sea with a horizontal resolution of 1/24 of a degree, which corresponds to about 4 km. The vertical dynamics in the current NEMO model setting are resolved on 141 unevenly spaced z* vertical levels. The vertical mixing is described through a Richardson number dependent formulation (Pacanowski and Philander, 1981). This formulation imposes an upper threshold to the vertical eddy coefficients fixed to 0.01 $m^2 s^{-1}$. However, an enhanced vertical diffusion parameterization is also applied. Therefore, where the squared Brunt Vaisala frequency is lower than 10^{-12} s^{-2}, the vertical eddy coefficients are assigned a larger value (enhanced vertical diffusivity). In the current setting, this value is fixed to 10 $m^2 s^{-1}$. The model equations explicitly include a tidal potential accounting for the main eight tidal components, namely M2, S2, K1, O1, N2, P1, Q1, and K2.

The initial conditions for the forecast are provided by analysis constructed with a data assimilation 3D-Var scheme, OceanVar (Dobricic and Pinardi, 2008), that assimilates along track sea level anomaly, vertical profiles of temperature and salinity from in situ data and corrects the non-solar heat fluxes through an SST relaxation based on satellite data. In this MedFS setting 39 rivers are implemented. The runoff is provided from the daily EFAS v5 dataset (Mazzetti et al., 2023). A fixed salinity value is attributed to each river mouth. The forecast is driven by the European Centre for Medium-range Weather Forecasts (ECMWF) atmospheric forecast fields, including mean sea level pressure, 10 m winds, 2 m temperature, dew point

https://doi.org/10.5194/egusphere-2026-4734
Preprint. Discussion started: 21 August 2026

temperature, precipitation, and cloud cover with a spatial resolution of 1/10 of a degree and a time resolution of 1 hour (for the first 3 days of forecast). The lateral open boundary conditions in the Atlantic Ocean and at the Dardanelles Strait are provided by the *Copernicus Marine Global Ocean Physics Analysis and Forecast* product (E.U. Copernicus Marine Service, 2026). Tidal amplitudes and velocities at the Atlantic boundary are imposed from FES2014 (Lyard et al., 2021) and TUGO models (Lynch and Gray, 1979). A Flather condition is used for the barotropic currents at the boundary, while the baroclinic ones are included through a flow relaxation scheme.

MedFS shows very good skills in representing the tides in terms of both amplitude and phase in the Adriatic Sea. Several validation metrics based on harmonic analysis results are used to validate each tidal component with respect to available observed and numerical results (Gualtieri et al., 2025). The results obtained from this version of the model, referred to as MedFS, are compared with a twin system version that does not include explicit tides, labelled MedFS-NT.

To better understand the baroclinic effects, we developed a barotropic model version called MedFS-BT. This NEMO 4.2 barotropic configuration consists of a single vertical layer, a constant density imposed over the whole domain, and a constant bottom friction drag coefficient set to 2.5×10^{-3}, used instead of the law of the wall logarithmic formulation. The same lateral open boundary conditions are prescribed for the barotropic flow at the Atlantic boundary. MedFS-BT is forced by the same atmospheric pressure and wind fields used in the MedFS. The wind stress drag coefficient is set to a constant value of 1.2×10^{-3}, which is consistent with the global mean estimate (Kara et al., 2007) and is commonly used in numerical experiments based on a constant drag coefficient formulation (Zedler et al., 2009).

The MedFS-NT forecast is initialized from a non-tidal analysis run started from the MedFS analysis on 1 October 2019, while the MedFS-BT forecast is initialized from a barotropic simulation forced by atmospheric analysis fields and started on the same date. In Table A1 the set of experiments used in this study is summarized.

Table A1. List of experiments

Experiment	System components	Explicit tides	Vertical levels	Atmospheric forcing spatial and temporal resolutions
MedFS	NEMO+WW3	Yes	141	1/10° 1 hour (ECMWF Forecast)
MedFS-NT	NEMO+WW3	No	141	1/10° 1 hour (ECMWF Forecast)
MedFS-BT	NEMO	Yes	1	1/10° 1 hour (ECMWF Forecast)

In a preliminary test, the sensitivity to atmospheric conditions was qualitatively assessed. A specific set of sensitivity experiments was carried out. Analysis and re-forecast system runs forced by available atmospheric forcings with a spatial resolution of 1/10 and 1/8 of a degree, as well as with atmospheric forcings with temporal resolutions of 1, 3, and 6 hours, were compared. These runs were performed with the settings of the MedFS with and without tides. The complete list of these preliminary tests is reported in Table A2. The table summarizes for each experiment the system components, the tidal setting,

https://doi.org/10.5194/egusphere-2026-4734
Preprint. Discussion started: 21 August 2026

the ECMWF atmospheric forcing details, and the sea level peak reached on 12 November 2019 at the ISMAR tide-gauge. The sea level peaks are obtained by applying to all the time series the same offset procedure described in Sect. 2 and, in the tests without explicit tides, the TPXO (Egbert and Erofeeva, 2002) tidal signal has been linearly added to the modelled sea level to allow a direct comparison with the corresponding tidal runs.

Table A2. List of preliminary sensitivity tests

Experiment	System components	Explicit tides	Atmospheric forcing details	Sea level peak at ISMAR tide-gauge on 12 Nov 2019
MedFS_FC_FCw10	NEMO+WW3	Yes	1/10° 1 hour (ECMWF Forecast)	157 cm
MedFS-NT_FC_FCw10	NEMO+WW3	No	1/10° 1 hour (ECMWF Forecast)	154 cm (TPXO tides added)
MedFS_AN_ANw10	NEMO+WW3+OceanVar	Yes	1/10° 6 hours (ECMWF Analysis)	136 cm
MedFS-NT_AN_ANw10	NEMO+WW3+OceanVar	No	1/10° 6 hours (ECMWF Analysis)	136 cm (TPXO tides added)
MedFS_FC_FCw08	NEMO+WW3	Yes	1/8° 3 hours (ECMWF Forecast)	125 cm
MedFS-NT_FC_FCw08	NEMO+WW3	No	1/8° 3 hours (ECMWF Forecast)	124 cm (TPXO tides added)
MedFS_AN_ANw08	NEMO+WW3+OceanVar	Yes	1/8° 6 hours (ECMWF Analysis)	136 cm
MedFS-NT_AN_ANw08	NEMO+WW3+OceanVar	No	1/8° 6 hours (ECMWF Analysis)	136 cm (TPXO tides added)

Data availability

The sea level observations recorded at the ISMAR tide-gauge are publicly available from the Venice Municipality website (https://www.comune.venezia.it/it/content/3-piattaforma-ismar-cnr, last access: 4 August 2026). The *Mediterranean Sea Physics Analysis and Forecast* product is distributed by the Copernicus Marine Service (E.U. Copernicus Marine Service, 2025). The experiments presented in this work were produced with the EAS9 version of this system (see Appendix A), and their outputs are available from the authors upon request.

Author contribution

A.C. Goglio carried out the experiments, coded and performed the post-processing, and prepared the draft of the manuscript. All the work was supervised by E. Clementi and N. Pinardi. P. Oddo provided scientific advice, support during the analysis and comments on the manuscript. G. Boccaletti contributed to the conception of the study and provided comments on the manuscript. L. Mentaschi provided scientific advice and support on the barotropic contributions analysis.

Competing interests

The authors declare that they have no conflict of interest.

https://doi.org/10.5194/egusphere-2026-4734
Preprint. Discussion started: 21 August 2026

Acknowledgements

A.C. Goglio gratefully acknowledges her PhD supervisors, Nadia Pinardi and Emanuela Clementi, and all co-authors for their guidance. This work was carried out at the CMCC Foundation (Euro-Mediterranean Center on Climate Change) in Bologna, Italy, and made use of the CMCC High-Performance Computing (HPC) infrastructure. Artificial intelligence tools were used for grammatical corrections, language refinement of the manuscript, and improvements to the formatting and visual consistency of the figures.

Financial support

This research was funded under the contract for the Mediterranean Sea Monitoring and Forecasting Centre (Contract No. 24252L05-COP-MFC MED-5200) within the Copernicus Marine Service, funded by the European Union, implemented by Mercator Ocean International, CUP n. C53C24001610006.

References

Arbic, B. K., Wallcraft, A. J., and Metzger, E. J.: Concurrent simulation of the eddying general circulation and tides in a global ocean model, Ocean Modell., 32, 175–187, https://doi.org/10.1016/j.ocemod.2010.01.007, 2010.

Arbic, B. K.: Incorporating tides and internal gravity waves within global ocean general circulation models: A review, Prog. Oceanogr., 206, 102824, https://doi.org/10.1016/j.pocean.2022.102824, 2022.

Bajo, M., Međugorac, I., Umgiesser, G., and Orlić, M.: Storm surge and seiche modelling in the Adriatic Sea and the impact of data assimilation, Q. J. R. Meteorol. Soc., 145, 2070–2084, https://doi.org/10.1002/qj.3544, 2019.

Boetti, M., Causio, S., Goglio, A. C., Clementi, E., Coppini, G., and Federico, I.: Model framework for storm surge forecasting in Venice Lagoon: what-if scenario with movable barriers, Front. Mar. Sci., 13, 1771571, https://doi.org/10.3389/fmars.2026.1771571, 2026.

Borile, F.: Towards a broader understanding of the effects of tidal forcing on the global ocean circulation, Ph.D. thesis, Alma Mater Studiorum Università di Bologna, https://doi.org/10.48676/unibo/amsdottorato/10329, 2022.

Cavaleri, L., Bajo, M., Barbariol, F., Bastianini, M., Benetazzo, A., Bertotti, L., Chiggiato, J., Ferrarin, C., Trincardi, F., and Umgiesser, G.: The 2019 flooding of Venice and its implications for future predictions, Oceanography, 33, 42–49, https://doi.org/10.5670/oceanog.2020.105, 2020.

Cid, A., Menéndez, M., Castanedo, S., Abascal, A. J., Méndez, F. J., and Medina, R.: Long-term changes in the frequency, intensity and duration of extreme storm surge events in southern Europe, Clim. Dynam., 46, 1503–1516, https://doi.org/10.1007/s00382-015-2659-1, 2016.

Coppini, G., Clementi, E., Cossarini, G., Salon, S., Korres, G., Ravdas, M., Lecci, R., Pistoia, J., Goglio, A. C., Drudi, M., Grandi, A., Aydogdu, A., Escudier, R., Cipollone, A., Lyubartsev, V., Mariani, A., Cretì, S., Palermo, F., Scuro, M., Masina, S., Pinardi, N., Navarra, A., Delrosso, D., Teruzzi, A., Di Biagio, V., Bolzon, G., Feudale, L., Coidessa, G., Amadio, C., Brosich, A., Miró, A., Alvarez, E., Lazzari, P., Solidoro, C., Oikonomou, C., and Zacharioudaki, A.: The Mediterranean Forecasting System – Part 1: Evolution and performance, Ocean Sci., 19, 1483–1516, https://doi.org/10.5194/os-19-1483-2023, 2023.

Davies, A. M. and Xing, J.: Influence of coastal fronts on near-inertial internal waves, Geophys. Res. Lett., 29, 2114, https://doi.org/10.1029/2002GL015904, 2002.

Dobricic, S. and Pinardi, N.: An oceanographic three-dimensional variational data assimilation scheme, Ocean Modell., 22, 89–105, https://doi.org/10.1016/j.ocemod.2008.01.004, 2008.

Dong, C., Xu, G., Han, G., Chen, N., He, Y., and Chen, D.: Identification of tidal mixing fronts from high-resolution along-track altimetry data, Remote Sens. Environ., 209, 489–496, https://doi.org/10.1016/j.rse.2018.02.047, 2018.

Egbert, G. D. and Erofeeva, S. Y.: Efficient inverse modeling of barotropic ocean tides, J. Atmos. Ocean. Technol., 19, 183–204, https://doi.org/10.1175/1520-0426(2002)019<0183:EIMOBO>2.0.CO;2, 2002.

E.U. Copernicus Marine Service: Mediterranean Sea Physics Analysis and Forecast, Mercator Ocean International [data set], https://doi.org/10.48670/mds-00359, 2025.

E.U. Copernicus Marine Service: Global Ocean Physics Analysis and Forecast, Mercator Ocean International [data set], https://doi.org/10.48670/moi-00016, 2026.

Faranda, D., Ginesta, M., Alberti, T., Coppola, E., and Anzidei, M.: Attributing Venice Acqua Alta events to a changing climate and evaluating the efficacy of MoSE adaptation strategy, npj Clim. Atmos. Sci., 6, 181, https://doi.org/10.1038/s41612-023-00513-0, 2023.

https://doi.org/10.5194/egusphere-2026-4734
Preprint. Discussion started: 21 August 2026

Ferrarin, C., Bajo, M., Benetazzo, A., Cavaleri, L., Chiggiato, J., Davison, S., Davolio, S., Lionello, P., Orlić, M., and Umgiesser, G.: Local and large-scale controls of the exceptional Venice floods of November 2019, Prog. Oceanogr., 197, 102628, https://doi.org/10.1016/j.pocean.2021.102628, 2021.

Ferrarin, C., Lionello, P., Orlić, M., Raicich, F., and Salvadori, G.: Venice as a paradigm of coastal flooding under multiple compound drivers, Sci. Rep., 12, 5754, https://doi.org/10.1038/s41598-022-09652-5, 2022.

Ferrarin, C., Orlić, M., Bajo, M., Davolio, S., Umgiesser, G., and Lionello, P.: The contribution of a mesoscale cyclone and associated meteotsunami to the exceptional flood in Venice on November 12, 2019, Q. J. R. Meteorol. Soc., 149(756), 2929–2942, https://doi.org/10.1002/qj.4539, 2023.

Giesen, R., Clementi, E., Bajo, M., Federico, I., Stoffelen, A., and Santoleri, R.: The November 2019 record high water levels in Venice, Italy, in: Copernicus Marine Service Ocean State Report, Issue 5, J. Oper. Oceanogr., 14, s156–s161, https://doi.org/10.1080/1755876X.2021.1946240, 2021.

Godlewski, G. B., Caporalini, L., and Deuss, B.: Acqua Alta and the need for the Mo.S.E. project, TU Delft student research project report, http://resolver.tudelft.nl/uuid:ea34a719-79c1-4c6e-b886-e0d92407bc9d, 2020.

Gualtieri, L., Goglio, A. C., Clementi, E., Grandi, A., Moulin, A., Giurato, M., Aydogdu, A., Pistoia, J., Miraglio, P., Sadighrad, E., Mariani, A., and Drudi, M.: EU Copernicus Marine Service Quality Information Document for the Mediterranean Sea Physical Analysis and Forecasting Product, MEDSEA_ANALYSISFORECAST_PHY_006_013, Issue 2.6, Mercator Ocean International, https://documentation.marine.copernicus.eu/QUID/CMEMS-MED-QUID-006-013.pdf, 2025.

Idier, D., Bertin, X., Thompson, P., and Pickering, M. D.: Interactions between mean sea level, tide, surge, waves and flooding: mechanisms and contributions to sea level variations at the coast, Surv. Geophys., 40, 1603–1630, https://doi.org/10.1007/s10712-019-09549-5, 2019.

Kara, A. B., Wallcraft, A. J., Metzger, E. J., Hurlburt, H. E., and Fairall, C. W.: Wind stress drag coefficient over the global ocean, J. Climate, 20, 5856–5864, https://doi.org/10.1175/2007JCLI1900.1, 2007.

Leonardi, N.: The barriers of Venice, Nat. Geosci., 14, 881–882, https://doi.org/10.1038/s41561-021-00864-4, 2021.

https://doi.org/10.5194/egusphere-2026-4734
Preprint. Discussion started: 21 August 2026

Lionello, P., Nicholls, R. J., Umgiesser, G., and Zanchettin, D.: Venice flooding and sea level: past evolution, present issues, and future projections (introduction to the special issue), Nat. Hazards Earth Syst. Sci., 21, 2633–2641, https://doi.org/10.5194/nhess-21-2633-2021, 2021a.

Lionello, P., Barriopedro, D., Ferrarin, C., Nicholls, R. J., Orlić, M., Raicich, F., Reale, M., Umgiesser, G., Vousdoukas, M., and Zanchettin, D.: Extreme floods of Venice: characteristics, dynamics, past and future evolution (review article), Nat. Hazards Earth Syst. Sci., 21, 2705–2731, https://doi.org/10.5194/nhess-21-2705-2021, 2021b.

Lyard, F. H., Allain, D. J., Cancet, M., Carrère, L., and Picot, N.: FES2014 global ocean tide atlas: design and performance, Ocean Sci., 17, 615–649, https://doi.org/10.5194/os-17-615-2021, 2021.

Lynch, D. R. and Gray, W. G.: A wave equation model for finite element tidal computations, Comput. Fluids, 7, 207–228, https://doi.org/10.1016/0045-7930(79)90037-9, 1979.

Madec, G. and the NEMO System Team: NEMO Ocean Engine Reference Manual, Zenodo, https://doi.org/10.5281/zenodo.8167700, 2023.

Marcos, M., Tsimplis, M. N., and Shaw, A. G. P.: Sea level extremes in southern Europe, J. Geophys. Res. Oceans, 114, C01007, https://doi.org/10.1029/2008JC004912, 2009.

Mazzetti, C., Carton De Wiart, C., Gomes, G., Russo, C., Decremer, D., Grimaldi, S., Disperati, J., Ziese, M., Schweim, C., Garcia Sanchez, R., Jacobson, T., Ramos, A., Prudhomme, C., and Salamon, P.: EFAS v5.0 hydrological reanalysis, European Commission, Ispra, JRC134686, 2023.

McDonagh, B., Clementi, E., Goglio, A. C., and Pinardi, N.: The characteristics of tides and their effects on the general circulation of the Mediterranean Sea, Ocean Sci., 20, 1051–1066, https://doi.org/10.5194/os-20-1051-2024, 2024.

McDonagh, B., von Storch, J.-S., Clementi, E., and Pinardi, N.: Internal tides in the Mediterranean Sea, Prog. Oceanogr., 241, 103647, https://doi.org/10.1016/j.pocean.2025.103647, 2026.

Mellor, G. L. and Wang, X.-H.: Pressure compensation and the bottom boundary layer, J. Phys. Oceanogr., 26, 2214–2222, https://doi.org/10.1175/1520-0485(1996)026<2214:PCATBB>2.0.CO;2, 1996.

Mellor, G. L.: Introduction to Physical Oceanography, American Institute of Physics, Melville, NY, 260 pp., 1996.

https://doi.org/10.5194/egusphere-2026-4734
Preprint. Discussion started: 21 August 2026

Oddo, P., Pinardi, N., and Zavatarelli, M.: A numerical study of the interannual variability of the Adriatic Sea (2000–2002), Sci. Total Environ., 353, 39–56, https://doi.org/10.1016/j.scitotenv.2005.09.061, 2005.

Pacanowski, R. C. and Philander, S. G. H.: Parameterization of vertical mixing in numerical models of tropical oceans, J. Phys. Oceanogr., 11, 1443–1451, https://doi.org/10.1175/1520-0485(1981)011<1443:POVMIN>2.0.CO;2, 1981.

Pawlowicz, R., Beardsley, B., and Lentz, S.: Classical tidal harmonic analysis including error estimates in MATLAB using T_TIDE, Comput. Geosci., 28, 929–937, https://doi.org/10.1016/S0098-3004(02)00013-4, 2002.

Pirazzoli, P. A.: Did the Italian Government approve an obsolete project to save Venice?, Eos Trans. AGU, 83, 217–223, https://doi.org/10.1029/2002EO000148, 2002.

Robinson, A. R., Tomasin, A., and Artegiani, A.: Flooding of Venice: phenomenology and prediction of the Adriatic storm surge, Q. J. R. Meteorol. Soc., 99, 688–692, https://doi.org/10.1002/qj.49709942210, 1973.

Stoffelen, A., Verspeek, J. A., Vogelzang, J., and Verhoef, A.: The CMOD7 geophysical model function for ASCAT and ERS wind retrievals, IEEE J. Sel. Top. Appl. Earth Obs. Remote Sens., 10, 2123–2134, https://doi.org/10.1109/JSTARS.2017.2681806, 2017.

Trincardi, F., Barbanti, A., Bastianini, M., Benetazzo, A., Cavaleri, L., Chiggiato, J., Papa, A., Pomaro, A., Sclavo, M., Tosi, L., and Umgiesser, G.: The 1966 flooding of Venice: What time taught us for the future, Oceanography, 29, 178–186, https://doi.org/10.5670/oceanog.2016.87, 2016.

Umgiesser, G. and Matticchio, B.: Simulating the mobile barrier (MOSE) operation in the Venice Lagoon, Italy: global sea level rise and its implication for navigation, Ocean Dynam., 56, 320–332, https://doi.org/10.1007/s10236-006-0071-4, 2006.

Umgiesser, G., Bajo, M., Ferrarin, C., Cucco, A., Lionello, P., Zanchettin, D., Papa, A., Tosoni, A., Ferla, M., Coraci, E., Morucci, S., Crosato, F., Bonometto, A., Valentini, A., Orlić, M., Haigh, I. D., Nielsen, J. W., Bertin, X., Fortunato, A. B., Pérez Gómez, B., Alvarez Fanjul, E., Paradis, D., Jourdan, D., Pasquet, A., Mourre, B., Tintoré, J., and Nicholls, R. J.: The prediction of floods in Venice: methods, models and uncertainty (review article), Nat. Hazards Earth Syst. Sci., 21, 2679–2704, https://doi.org/10.5194/nhess-21-2679-2021, 2021.

Vilibić, I. and Orlić, M.: Surface seiches and internal Kelvin waves observed off Zadar (East Adriatic), Estuar. Coast. Shelf Sci., 48, 125–136, 1999.

https://doi.org/10.5194/egusphere-2026-4734
Preprint. Discussion started: 21 August 2026

Vilibić, I., Leder, N., and Smirčić, A.: Forced and free response of the Adriatic Sea level, Nuovo Cimento C, 21, 439–451, 1998.

Wang, P., Bernier, N. B., Thompson, K. R., and Kodaira, T.: Evaluation of a global total water level model in the presence of radiational S2 tide, Ocean Model., 168, 101893, https://doi.org/10.1016/j.ocemod.2021.101893, 2021.

Wang, P., Bernier, N. B., and Thompson, K. R.: Adding baroclinicity to a global operational model for forecasting total water level: approach and impact, Ocean Modell., 174, 102031, https://doi.org/10.1016/j.ocemod.2022.102031, 2022.

WaveWatch III Development Group: User manual and system documentation of WAVEWATCH III® version 6.07, Tech. Note 333, NOAA/NWS/NCEP/MMAB, College Park, MD, USA, 465 pp. + Appendices, 2019.

Williams, J., Horsburgh, K. J., Williams, J. A., and Proctor, R. N. F.: Tide and skew surge independence: new insights for flood risk, Geophys. Res. Lett., 43, 6410–6417, https://doi.org/10.1002/2016GL069522, 2016.

Woodworth, P. L., Melet, A., Marcos, M., Ray, R. D., Wöppelmann, G., Sasaki, Y. N., Cirano, M., Hibbert, A., Huthnance, J. M., Monserrat, S., and Merrifield, M. A.: Forcing factors affecting sea level changes at the coast, Surv. Geophys., 40, 1351–1397, https://doi.org/10.1007/s10712-019-09531-1, 2019.

Zavatarelli, M. and Pinardi, N.: The Adriatic Sea modelling system: a nested approach, Ann. Geophys., 21, 345–364, https://doi.org/10.5194/angeo-21-345-2003, 2003.

Zedler, S. E., Niiler, P. P., Stammer, D., Terrill, E., and Morzel, J.: Ocean's response to Hurricane Frances and its implications for drag coefficient parameterization at high wind speeds, J. Geophys. Res. Oceans, 114, C04016, https://doi.org/10.1029/2008JC005205, 2009.